Prediction of complex atrioventricular conduction rhythms in humans with use of the atrioventricular nodal recovery curve

ALVIN SHRIER, PH.D., HOWARD DUBARSKY, B.SC., MICHAEL ROSENGARTEN, M.D., MICHAEL R. GUEVARA, PH.D., STANLEY NATTEL, M.D., AND LEON GLASS, PH.D.

ABSTRACT Theoretical considerations indicate that complex patterns of atrioventricular conduction produced by rapid atrial stimulation can be predicted from changes in atrioventricular conduction produced by premature stimulation of the atrium. The purpose of this study was to evaluate the validity of this theoretical approach in seven patients undergoing electrophysiologic investigation. The atrioventricular nodal recovery curve was determined at two different basic cycle lengths. Subsequently, periodic atrial stimulation was delivered for 30 sec periods over a range of frequencies giving 11, Wenckebach, reverse Wenckebach, and 21 rhythms. The recovery curve data was then used to compute the response to periodic stimulation by an iterative technique. The conduction patterns actually seen during periodic atrial stimulation showed close agreement with the computed patterns. This work thus provides a unified explanation for the appearance of Wenckebach, reverse Wenckebach, alternating Wenckebach, and high grade block rhythms.
Circulation 76, No. 6, 1196–1205, 1987.

THE ELECTROPHYSIOLOGIC mechanisms underlying the generation of the various rhythms seen during atrioventricular block are unclear. Different mechanisms are generally thought to be responsible for various rhythms, such as Wenckebach,[1, 2] reverse Wenckebach,[3, 4] alternating Wenckebach,[5, 6] and Mobitz type II[7] atrioventricular block. It has recently been shown that patterns resembling many of these rhythms of atrioventricular block can be seen in a virtually isopotential preparation of cardiac cells; moreover, the existence of these patterns can be predicted by analyzing the response of the preparation to premature stimulation.[8–10] Indeed, very similar theoretical methods were initially used in the study of atrioventricular block.[11–14] This study demonstrates that various rhythms of atrioventricular block seen in patients during 30 sec periods of atrial stimulation can be largely accounted for by the response of the atrioventricular node to premature stimulation, as described by the atrioventricular nodal recovery curve.[15–19]

From the Departments of Physiology, Pharmacology, and Medicine, McGill University, the Division of Cardiology, Montreal General Hospital, and the Department of Medicine, Montreal Heart Institute, Montreal, Quebec, Canada.

Supported by grants from The Canadian Heart Foundation and the Medical Research Council of Canada.

Address for correspondence: Alvin Shrier, PH.D., Department of Physiology, McGill University, 3655 Drummond St., Montreal, Quebec, Canada, H3G 1Y6.

Received July 28, 1986; revision accepted Aug. 6, 1987.

Methods

Patients (table 1) undergoing electrophysiologic evaluation for suspected cardiac arrhythmias were considered suitable candidates for this study. All were in sinus rhythm with normal atrioventricular conduction as determined by electrocardiographic (ECG) criteria.[20] None of the patients chosen for study had bundle branch block and ventricular or atrial extrasystoles. Medications for each patient are listed in table 1. All patients were advised of the nature of the study and informed consent, as well as Ethics Committee approval, were obtained.

Right heart catheterization was performed on patients in the supine position who had been given 5 to 10 mg diazepam. Under local anaesthesia, a bipolar electrode catheter was percutaneously introduced into the right femoral vein and fluoroscopically positioned across the tricuspid valve. The catheter was slowly withdrawn until a sharp His bundle deflection appeared between the atrial and ventricular deflections.[21] Multiple surface ECG leads (I, II, III, and V_1) and the bipolar His bundle electrogram (HBE) were simultaneously monitored and recorded on a multichannel oscilloscopic photographic recorder (Honeywell VR-12) at a paper speed of 25 or 50 mm/sec. The HBE and surface ECGs were band-pass filtered (50 to 500 Hz and 0.1 to 250 Hz, respectively).

A quadripolar electrode catheter was also introduced percutaneously into the right femoral vein and fluoroscopically positioned in the region of the right atrial appendage. Two of the electrode poles were used to sense atrial depolarization and the remaining two were used to pace or deliver isolated test stimuli. A programmable battery-powered stimulator (Medtronic 5225)

TABLE 1
Electrophysiologic profile of patients

Patient no.	History	Medications	Spontaneous heart interval (msec)	PR interval (msec)	WB point (msec)	2:1 point (msec)	BCL (msec)	AH/HV HBE continuous	SH_{min} (msec)	α (msec)	τ (msec)	θ (msec)
1	Syncope	Isosorbide dinitrate, chlorpropamide, aspirin	800	150	355	280	750	No	178	326	88.7	76.2
							351		256	138	44.4	18.6
2	Syncope	Docusate sodium	800	200	360	270	750	No	233	125	97.9	67.0
							400		267	674	12.1	18.0
3	Syncope	—	800	180	370	300	800	Yes	114	383	252	113
							400		196	181	163	0
4	Syncope	Beclomethasone, nifedipine, theophylline	760	160	530	360	600	No	163	172	246	216
							531		168	1704	87	197
5	Palpitations	Nadolol, allopurinol, colchicine	1100	200	560	370	1000	No	243	987	59.8	129
							600		271	4735	46.3	125
6	Syncope	—	1090	190	500	350	896	Yes	250	1661	658	125
							800		[A]	[A]	[A]	133
7	Sinus bradycardia	—	1100	200	395	320	1000	Yes	182	810	140	154
							440		[B]	[B]	[B]	50

The minimum HS interval for which conduction occurs (θ) is 0 for patient 3 at BCL = 400 msec because the last stimulus to conduct, S, is introduced concurrently with the His deflection, H, of the preceding cycle.

WB point = longest interstimulus interval SS at which the Wenckebach rhythm is encountered; 2:1 point = longest interstimulus interval at which the 2:1 rhythm is encountered; SH_{min}, θ, α, and τ are positive constants used in equations 1A and 1B.

These recovery curves were fit with double exponentials as in equation 1B: [A]$SH = 147 + 1185 \exp\left[\frac{-HS}{53}\right] + 144 \exp\left[\frac{-HS}{687}\right]$; [B]$SH = 191 + 14455 \exp\left[\frac{-HS}{11}\right] + 161 \exp\left[\frac{-HS}{341}\right]$.

was used to deliver 2 msec pulses at twice diastolic threshold current.

Surface ECGs were initially recorded for 30 sec. The right atrium was then paced at a continuously increasing rate to obtain an estimate of the Wenckebach point, the cycle length at which 11 atrioventricular conduction was no longer possible and Wenckebach cycles appeared. For determination of the atrioventricular nodal recovery curve, the right atrium was captured and driven at one of two basic cycle lengths (BCLs). One rate was slightly more rapid than the spontaneous rate and the second rate was just lower than that at which Wenckebach cycles appeared. Once a steady-state in the AH interval was established at each pacing rate, single test stimuli were introduced into the atrium at progressively decreasing coupling intervals (S_1-S_2) after every eighth beat. The coupling interval was decreased in steps of 50 msec for coupling intervals greater than 500 msec, 20 msec for intervals between 300 and 500 msec, and 10 msec for intervals less than 300 msec.

After determination of the atrioventricular nodal recovery curve the right atrium was paced in most cases at nine different rates, all higher than the spontaneous rate; these rates were chosen so that four rates produced 11 rhythm, another four rates produced Wenckebach or reverse Wenckebach rhythms, and one rate produced a 21 rhythm. A periodic rhythm consisting of N atrial beats and M ventricular beats is called an NM rhythm, and the ratio M/N is termed the conduction ratio (CR). Thus, a maintained 43 rhythm has a conduction ratio of ¾. At each pacing rate recording was carried out for 30 sec. During most pacing intervals there was a mixture of rhythms. During a given pacing interval the CR was computed by dividing the number of ventricular beats by the number of atrial beats. This protocol was carried out in seven patients; in three of these seven patients HBEs were continuously recorded, while in the others the HBE could not be maintained throughout the entire recording period (table 1).

All records were hand-digitized on a graphics tablet (Hewlett-Packard 9111A). Measurements of data recorded at 25 mm/sec were repeatable to within ±10 msec. Records of the surface ECGs were used to determine spontaneous heart rate and atrioventricular conduction time of each patient. The HBE was used to quantitate atrioventricular nodal conduction (see figure 2): the coupling interval (S_1-S_2) was measured from the last stimulus artifact of the basic drive (S_1) to the test stimulus artifact (S_2), the recovery time (H_1-S_2) was measured from the last regular His bundle deflection (H_1) to the test stimulus artifact, and the atrioventricular nodal conduction time (S_2-H_2) was measured from the test stimulus artifact to the His bundle deflection in response to the test stimulus (H_2). The latency from the stimulus to the onset of the atrial electrogram was constant, allowing use of the more easily identified stimulus artifact as an event marker. In cases in which the His bundle deflection was not available, the initial R wave deflection was used instead of the His bundle signal in the analysis. The HV interval remained constant under the above stimulation protocols.

The atrioventricular nodal recovery curves were constructed by plotting the conduction time of the test beat (S_2-H_2) as a function of the preceding recovery time (H_1-S_2).[16, 17, 19] To simplify notation we drop the subscripts and hyphens and represent S_2-H_2 by SH and H_1-S_2 by HS. The atrioventricular nodal recovery curves were fitted to either a single or double exponential equation

$$SH = SH_{min} + \alpha \exp\left[\frac{-HS}{\tau}\right], \text{ for } HS \geq \theta \quad (1a)$$

or

$$SH = SH_{min} + \alpha_1 \exp\left[\frac{-HS}{\tau_1}\right] + \alpha_2 \exp\left[\frac{-HS}{\tau_2}\right], \text{ for } HS \geq \theta \quad (1b)$$

where SH_{min} is the minimum SH interval; α, α_1, α_2, and τ_1 and τ_2 are positive constants; and θ is the minimum HS interval for which conduction occurs.

The double exponential fit was chosen if the ratio of the sum of squared residuals for the double exponential fit was one-third or less of that for the single exponential fit. This was found to be the case in only two of the 14 fits performed for the seven patients studied. The values for the terms in equations 1a and 1b for each patient are listed in table 1.

Iterative technique. Once the recovery curve was characterized for a given patient, the effects of periodic stimulation at any frequency could be theoretically predicted with use of an iterative procedure. To do this equations must be generated, called finite-difference equations, by combining parameters from recovery curves 1a or 1b (e.g., SH_{min}, α, and τ) and the interval between atrial stimuli (SS). A schematic representation of periodic stimulation is shown in figure 1, which also introduces the relevant terminology. We made two basic assumptions: first, that the interval between stimuli (SS) is constant and second, that the atrioventricular conduction time after a given stimulus (SH_{i+1}) is a function *only* of the preceding recovery time (HS_i). Applying equation 1a we find that during periodic stimulation we can predict the conduction time from

$$SH_{i+1} = SH_{min} + \alpha_1 \exp\left[\frac{-HS_i}{\tau}\right] \quad (2)$$

Since HS_i is determined by SH_i and SS (see figure 1), we can write

$$HS_i = K(SS) - SH_i \quad (3)$$

where K is the smallest positive integer such that $K(SS) - SH_i \geq \theta$. Thus, K-1 represents the number of blocked atrial beats.

By substituting equation 3 into equation 2 we find

$$SH_{i+1} = SH_{min} + \alpha \exp\left[\frac{-(K(SS) - SH_i)}{\tau}\right] \quad (4a)$$

This finite-difference equation can be used to predict the rhythms observed during pacing at any stimulation frequency when a single exponential curve is used to fit the atrioventricular nodal recovery data. To do this we have to assume an arbitrary conduction time for the first paced beat (SH_1) and then compute (iterate) the conduction times for the subsequent paced beats (SH_2, SH_3. . . .) using equation 4a. For the form of the recovery curve found here, the asymptotic dynamics does not depend on the choice of SH_1.[27] In fact, in this study we set SH_1 equal to SH_{min}. The values for SH_{min}, α, and τ in equation 4a are obtained from equation 1a. Similarly, with the double-exponential formula for the atrioventricular nodal recovery curve we derive

$$SH_{i+1} = SH_{min} + \alpha_1 \exp\left[\frac{-(K(SS) - SH_i)}{\tau_1}\right] + \alpha_2 \exp\left[\frac{-(K(SS) - SH_i)}{\tau_2}\right] \quad (4b)$$

This finite-difference equation is used when the double exponential curve is chosen to fit the recovery data. Computations are carried out by setting $SH_i = SH_{min}$ and using values for α_1, τ_1, α_2, and τ_2 from equation 1b.

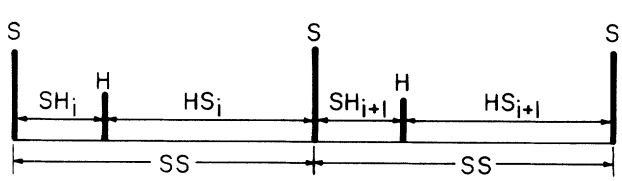

FIGURE 1. Schematic representation of periodic stimulation. Atrial stimulation artifacts (S), drawn at a constant atrial pacing interval (SS) give rise to His bundle deflections (H). The atrioventricular nodal conduction time (SH) and recovery time (HS) are shown.

Results

Atrioventricular nodal recovery curve. Figure 2 shows electrographic recordings and corresponding atrioventricular nodal recovery curves for one patient. Figure 2, *A*, shows the HBE when the right atrium was paced at a BCL of 1000 msec. As S_1-S_2 was decreased, there was a reduction in H_1-S_2 and a gradual prolongation in S_2-H_2 until eventually a critical value of S_1-S_2 was reached at which the cardiac impulse fails to traverse the atrioventricular node. The state of recovery of the atrioventricular node can be represented in the form of a recovery curve produced by plotting the conduction time (S_2-H_2) as a function of the preceding recovery time (H_1-S_2). Recovery curves obtained from this patient at two dierent values of BCL are shown in figure 2, *B*. One BCL (1000 msec) was slightly less than the spontaneous sinus interval of the patient and the second BCL (440 msec) was larger than the BCL at which Wenckebach cycles were first observed. In both cases, as the stimulus interval (S_1-S_2) decreased there was a concomitant reduction in the recovery time (H_1-S_2) and an increase in the conduction time (S_2-H_2). According to the criteria discussed above, the data in figure 2 obtained at a BCL of 1000 msec was fit by a single exponential equation, whereas the data obtained at a BCL of 440 msec were fit by a double exponential equation.

Rhythms of atrioventricular nodal conduction. In response to atrial pacing, 1:1, Wenckebach, reverse Wenckebach, and 2:1 rhythms were observed. When a 1:1 rhythm was seen, the SH interval progressively increased as the pacing frequency was increased until a critical pacing frequency was reached at which Wenckebach rhythms containing dropped beats resulted. Increasing the stimulation rate even further produced higher order Wenckebach rhythms and finally a 2:1 rhythm.

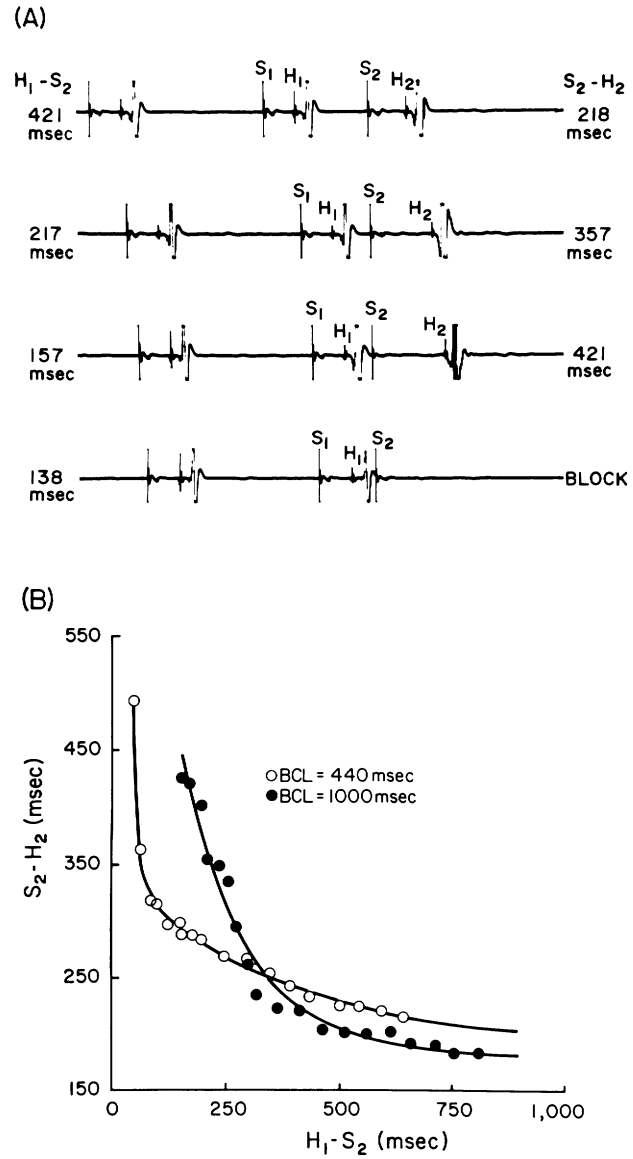

FIGURE 2. *A*, HBE at four different values of S_1-S_2 with a BCL of 1000 msec in patient 7. S_1 is the basic drive stimulus artifact, H_1 is the His bundle deflection in response to S_1, S_2 is the test stimulus artifact, and H_2 is the His bundle deflection in response to S_2. *B*, Atrioventricular nodal recovery curves at two different stimulation rates in patient 7. Atrioventricular nodal conduction time (S_2-H_2) is plotted as a function of the preceding recovery time (H_1-S_2). Filled circles were obtained with BCL = 1000 msec and open circles with BCL = 440 msec. With BCL = 1000 msec, SH = 182 + 810 exp[-HS/140]; with BCL = 440 msec, SH = 191 + 14455 exp[-HS/11] + 161 exp[-HS/341].

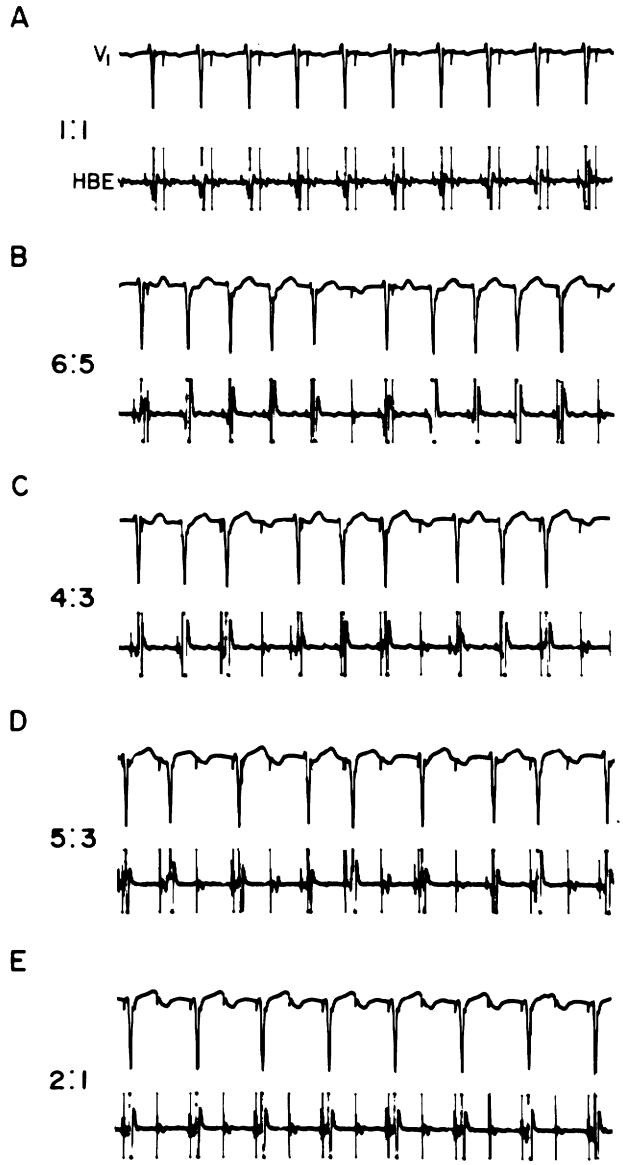

FIGURE 3. Representative examples of 1:1 conduction, Wenckebach and reverse Wenckebach periodicity, and 2:1 rhythm from patient 7. HBEs are shown at five different SS values. *A*, SS = 462 msec, 1:1 conduction; *B*, SS = 393 msec, 6:5 conduction; *C*, SS = 384 msec, 4:3 conduction; *D*, SS = 357 msec, 5:3 conduction; *E*, SS = 310 msec, 2:1 conduction.

Representative examples of simultaneous ECG and HBE recordings demonstrating 1:1, Wenckebach, reverse Wenckebach, and 2:1 rhythms are shown in figure 3. These tracings were taken from the same patient whose recovery curves are shown in figure 2. In figure 3, *A*, 1:1 atrioventricular conduction is shown: there was very little change in the SH and HS times from beat to beat. This was found for all stimulation rates producing 1:1 conduction. For the atrioventricular nodal rhythms shown in figure 3, *B* and *C*, there is Wenckebach periodicity—a progressive lengthening of the SH interval within any Wenckebach cycle with a concomitant reduction in the HS interval until a dropped beat occurs. For both the 6:5 and 4:3 Wenckebach rhythms, the shortest SH interval is seen in the first complex after the dropped beat. A complex 5:3 reverse Wenckebach rhythm composed of alternating 3:2 and 2:1 cycles could also be observed for short periods of time in this patient (figure 3, *D*). Finally, 2:1 atrioventricular block occurred as shown in figure 3, *E*. The absence of a His bundle deflection

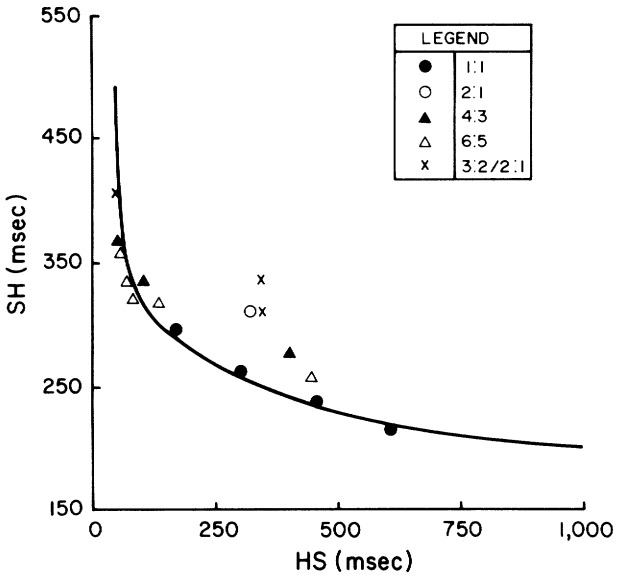

FIGURE 4. Atrioventricular nodal conduction time as a function of the preceding recovery time during periodic stimulation in patient 7. The recovery curve shows the relationship between the SH and HS intervals at a BCL of 440 msec as in figure 2. The legend indicates the various rhythms encountered during periodic stimulation. The points represent the mean SH and HS values taken at each stimulation rate from between eight cycles, for the 6:5 rhythm, up to 30 cycles, for the 2:1 rhythm. The SEM (not shown) ranges between 2.4 and 11.6 msec. 1:1 conduction was recorded at four atrial pacing lengths greater than 440 msec and Wenckebach periodicity was recorded at four atrial pacing cycle lengths less than 440 msec. For each rhythm with blocked beats the data point that occurs with the greatest value of HS corresponds to the first conducted beat after a blocked beat. Note that these points tend to cluster above the SH-HS curve. The designation 3:2/2:1 means that both 3:2 and 2:1 rhythms were seen at the value of SS.

after the atrial deflections in figure 3, *B* to *E*, indicates that conduction block occurred proximal to the His bundle.

The mean SH and HS intervals recorded at these stimulation rates are illustrated graphically in figure 4, where atrioventricular nodal conduction time (SH interval) is plotted vs the preceding recovery time (HS interval). The recovery curve obtained at a BCL of 440 msec, which is just above the Wenckebach point, is also plotted. The majority of the data points plotted in figure 4 fall very close to the recovery curve. This indicates that for an equivalent HS interval, the SH interval in response to periodic stimulation is similar to the SH interval found during premature stimulation. However, other points lie above the recovery curve: these correspond to the relatively prolonged SH intervals of conducted beats immediately after dropped beats in the Wenckebach and 2:1 zones. These points thus represent conduction times that are longer than those predicted by the recovery curve.

Assuming that the recovery curve gives the response of the atrioventricular node during periodic stimulation of the atrium, then equation 4a or 4b can be used to predict atrioventricular nodal conduction times at any given pacing frequency. The successive values of SH_i can be readily calculated from equation 4 on a digital computer. However, as Mobitz recognized in 1924,[11] such equations can also be solved graphically. Since this graphic iteration procedure is straightforward and gives insight into the dynamics of atrioventricular block, we now provide a description. If SH_{i+1} is plotted as a function of SH_i with use of equation 4a for a value of SS just 200 msec less than the intrinsic sinus cycle length (SS = 600 msec), the result is as shown in figure 5, *A*. The value SH* at which $SH_{i+1} = SH_i$ is called a steady state. The dashed path shows successive values of SH obtained if a periodic stimulus is initiated at $HS = \theta$, which is the longest possible HS interval. Successive values of SH decrease as the steady-state SH* is approached. Figure 5, *B*, shows that at a somewhat shorter SS interval (SS = 480 msec) the graph is transformed and shifted upward so that the steady-state SH* is at a longer SH interval. The dashed line again shows the graphically calculated successive values of SH. Note that the SH_i increases in this instance. Figure 5, *A* and *B*, shows that the steady-state values of the SH interval increase as the pacing interval SS decreases in the 1:1 region. As SS decreases further (figure 5, *C*) there is eventually no longer a steady state. Instead, there are now two branches of the SH_{i+1} vs SH_i curve. For the upper branch ($SH_i \leq SS - \theta$) there will be a conducted beat (K = 1) and a subsequent recovery time given by $SS - SH_i$. For the lower branch ($SH_i < SS - \theta$) there will be a blocked beat (K = 2), a longer recovery time ($2SS - SH_i$), and a correspondingly smaller value for SH_{i+1}. Graphic iteration leads to a stable cycle after a transient (not shown). In this case the cycle corresponds to a 4:3 Wenckebach rhythm with two iterates on the left branch of the curve, one iterate on the right branch, and successively increasing values of SH over the course of the cycle. The successive values of the SH intervals can be read directly from the graph and are in this case 168, 261, and 326 msec. Figure 5, *D* (SS = 360 msec), shows a 3:2 rhythm with alternating SH intervals of 308 and 189 msec. Figure 5, *E* (SS = 320 msec), shows a 5:3 rhythm with SH intervals of 342, 232, and 190 msec. This rhythm can be thought of as being composed of two consecutive 2:1 cycles followed by a 1:1 cycle and is thus complementary to the 4:3 rhythm (as has been previously noted by Roberge and Nadeau[4]). This rhythm also displays decreasing SH intervals that are

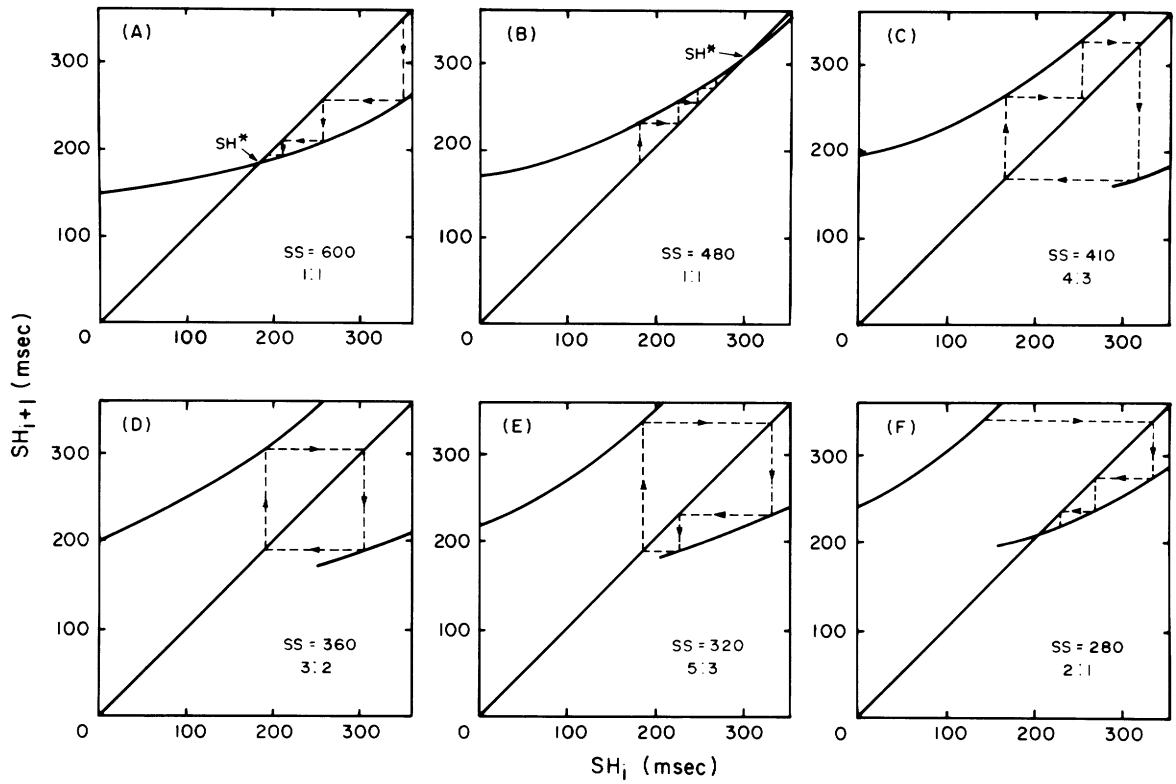

FIGURE 5. Graphic solution of equation 4a showing the dynamics for five different values of the pacing cycle length SS using the recovery curve determined at a BCL of 800 msec. The diagonal line is the line of identity $SH_{i+1} = SH_i$. *A*, SS = 600 msec, 1:1 conduction; *B*, SS = 480 msec, 1:1 conduction; *C*, SS = 410 msec, 4:3 conduction; *D*, SS = 360 msec, 3:2 conduction; *E*, SS = 320 msec, 5:3 conduction; *F*, SS = 280 msec, 2:1 conduction. Compare this with figures 7 to 16 from ref. 11. Data are from patient 3.

typical of reverse Wenckebach rhythms (see also figure 3, *D*). Finally, as illustrated in figure 5, *F* (SS = 280 msec), a stable 2:1 rhythm is established.

Figure 3, *B*, shows a 6:5 rhythm recorded in one patient at SS = 393 msec. Figure 6 demonstrates that a 6:5 rhythm is indeed predicted to occur in that patient at SS = 393 msec. Note that the increment in the SH interval decreases in the early part of the Wenckebach cycle, but then increases later on in the cycle. This late increase in the increment produces a decrement in the RR interval: such a predicted decrement can actually be seen in the patient (figure 3, *B*), resulting in atypical Wenckebach periodicity.

By use of this iterative procedure it was possible to determine the dynamics for any value of SS. For any N:M (N≥M) rhythm selected (when N,M are positive integers of 1 or greater and are relatively prime), a range of values of SS can be found that generates that rhythm. In figure 7, *A*, we plotted the CR as a function of SS. In figure 7, *B*, is shown an enlargement of the boxed region indicated in figure 7, *A*. In figure 7, as SS is progressively shortened there is a transition in the predicted rhythm from 1:1 to various Wenckebach rhythms to 2:1 rhythm. In addition to the usual N+1:N Wenckebach rhythms, more complex Wenckebach rhythms consisting of combinations of adjacent N+1:N Wenckebach cycles can also be found. These more complex Wenckebach rhythms are found between any two Wenckebach rhythms. For example, in between the 3:2 and 2:1 zones there is a range of SS for which a 7:4 rhythm is predicted.

The CRs recorded during periodic stimulation were then compared with the CRs theoretically predicted from the recovery curves recorded at the two different BCLs. The results from all seven patients are shown in figure 8. In each panel the CRs observed during periodic stimulation were plotted together with the theoretically predicted dynamics. The sequences of conduction patterns predicted agreed closely with those actually seen in the patients. In patients 3 and 7 (panels *C* and *G*) there was a large difference between the theoretically computed CRs at the two BCLs. This difference was due to the large differences in the effective refractory period (>100 msec) at the two different BCLs (see the parameter θ in table 1). As a consequence of this BCL dependence of the refractory period, a rhythm calculated to be at the left-hand border of the 1:1 region with the high-frequency nodal recovery

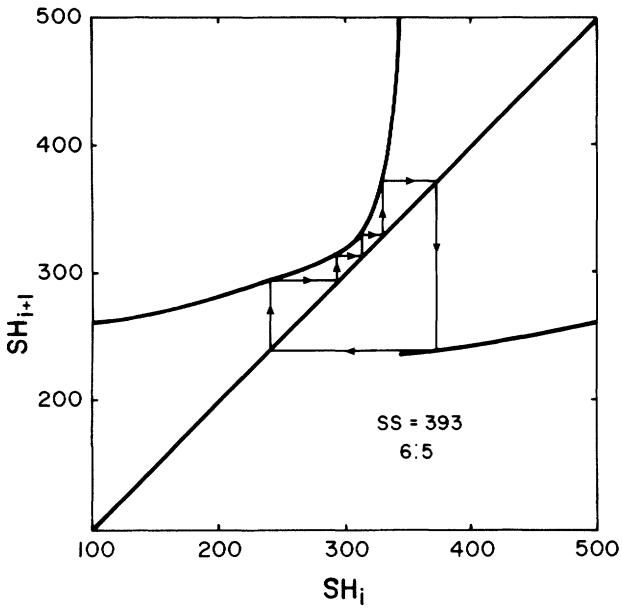

FIGURE 6. Graphic solution of equation 4b for SS = 393 msec. A 6:5 rhythm is predicted, with an increase in the increment of SH during the last beat of the Wenckebach cycle. Compare with figure 3, *B*. Data are from patient 7.

curve will be replaced by a Wenckebach rhythm if the low-frequency recovery curve is used instead. In patients 1 and 2 the differences in refractory periods were less (about 50 msec) and the tendency for separation in the computed CRs was less striking but still observable. In patients 4, 5, and 6, who showed small differences in refractory periods (<20 msec) with the high- and low-frequency stimulation rates, there was not a marked difference between the two computed sets of CRs. In general, an observed CR is found at a pacing interval SS that lies within 50 msec of the range of values of SS over which it is theoretically computed to exist by use of the high-frequency recovery curve.

Discussion

Many mechanisms have been proposed to explain Wenckebach periodicity.[1, 2] These include frequency-dependent decremental conduction,[22] modulation of an atrioventricular nodal oscillator by the sinus rhythm,[4] and a one-step delay at a discrete refractory barrier in the atrioventricular node.[23] These primary mechanisms may also be influenced by secondary factors such as accumulation of potassium ions or other ionic modifications associated with fatigue.[2] The iterative technique that we use is insensitive to the precise cellular mechanism(s) underlying atrioventricular nodal conduction: it is a simple iterative approach, relying on functional input/output aspects of the atrioventricular node described by its recovery curve. Indeed, use of the atrioventricular nodal recovery curve to predict rhythms of atrioventricular conduction goes back at least to Mobitz[11] (compare figures 7 to 16 of ref. 11 with figure 5 here); subsequently, several other investigators have independently rediscovered the technique.[10, 12, 13, 24–27] The present work represents the first systematic quantitative test of the hypothesis that the atrioventricular nodal recovery curve can be used to predict conduction patterns through the atrioventricular node during relatively brief (30 sec) periods of rapid atrial pacing.

Studies of a simple mathematical model of atrioventricular nodal conduction were undertaken by Landahl and Griffeath[26] and Keener.[27] The mathematical results of Keener can be applied to the iterative technique when the atrioventricular nodal recovery curve displays a single or double exponential decay (equation 1); more generally, they hold for any monotonically decreasing atrioventricular nodal recovery curve. Briefly, Keener[27] has shown that provided one has such a curve and the iterative scheme of equation 4 is valid, then if there is an N:M rhythm at one frequency and an N′:M′ rhythm at a second frequency there will be an N+N′:M+M′ rhythm at some intermediate frequency.

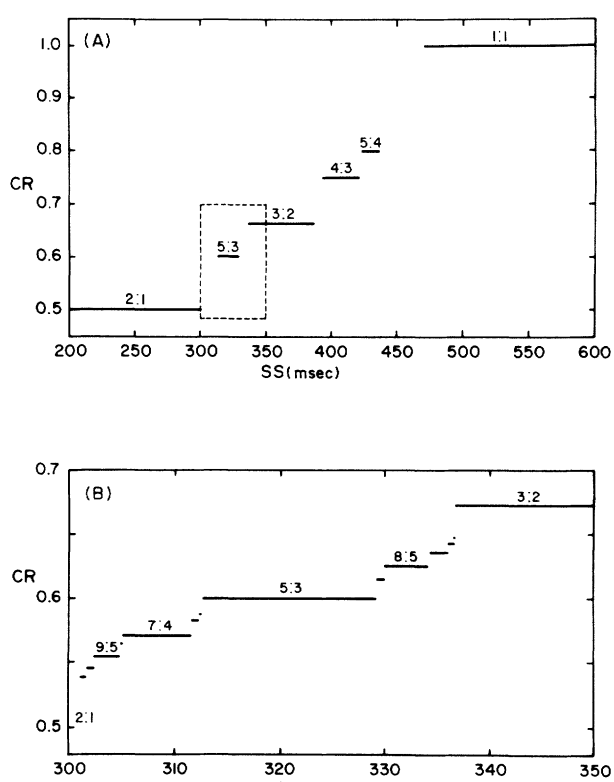

FIGURE 7. Theoretically computed CR plotted as a function of atrial pacing interval SS. *A*, SS is between 200 and 600 msec. *B*, Enlarged region from *A*. This function is sometimes called a Cantor function or devil's staircase.[31] Data are from patient 7.

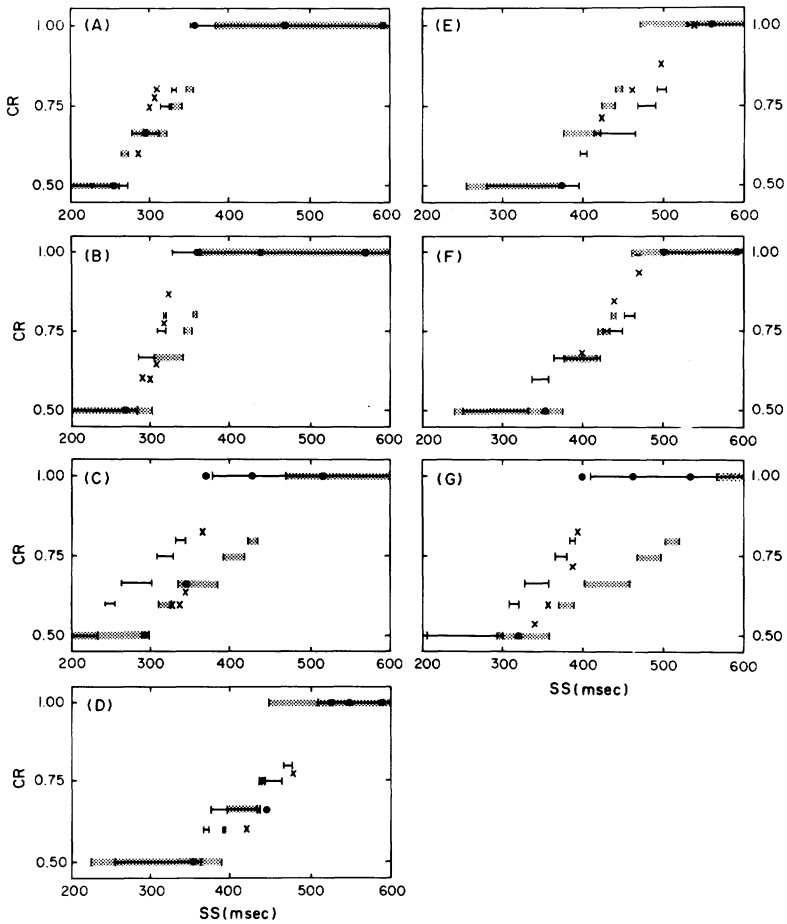

FIGURE 8. Composite showing the CR as a function of SS for the seven patients. The theoretically computed CRs were generated with the use of parameters listed in table 1 for the high-frequency stimulation recovery curves (solid line) and the low-frequency stimulation recovery curves (stippled lines). Symbols represent points determined during periodic stimulation of the atrium. Solid circles represent stable rhythms, whereas crosses represent complex or fluctuating rhythms. Panels *A* through *G* correspond to patients 1 through 7.

One implication of the mathematical analysis is that between the 1:1 and 2:1 conduction zones one expects to find stimulation frequency ranges that generate all the Wenckeback rhythms of the form N:N-1 (with $1 < N/(N-1) \leq 2$), as well as more complex rhythms such as 5:3, 7:4, and 8:5 rhythms. This is an important observation since it is frequently assumed that different mechanisms underlie Wenckebach, reverse Wenckebach, and alternating Wenckebach rhythms.[1-6] In fact, our results demonstrate that the existence of such rhythms is predicted (albeit only over narrow frequency ranges that may be difficult to observe in practice) during periodic stimulation of any individual displaying a monotonically decreasing atrioventricular nodal recovery curve. Thus, as initially pointed out by Decherd and Ruskin[12] in 1946, a single unified theory can serve to account for a very broad range of observations. For example, "millisecond Wenckebach"[28] is predicted to occur at an atrial rate just higher than that allowing 1:1 conduction, and the transient reverse Wenckebach recently observed by Young et al.[23] can be associated with the transient approach to a pattern of stable 1:1 conduction (figure 5, *A*). Stable reverse Wenckebach 5:3 rhythms[3, 4] are also theoretically predicted (figures 5, 7, and 8) and were observed in five of seven patients (figure 8). The fact that reverse Wenckebach rhythms are predicted to exist over only a narrow range of SS intervals (figures 7 and 8) might well account for their relative rarity. In addition, while multilevel block might account for some alternating Wenckebach rhythms,[5, 6] many forms of complex behavior can be predicted without the explicit incorporation of multiple levels of block into the model. Finally, note that one form of atypical Wenckebach periodicity seen in our patients (figure 3, *B*) is nicely predicted from the recovery curve (figure 6, see also ref. 14); in fact, atypical periodicity appears to be more common clinically then typical periodicity.[29]

The iterative approach requires certain assumptions known to be oversimplifications. The assumption that the SH interval depends solely on the preceding HS interval is an oversimplification. Lewis and Master[15] demonstrated more than 60 years ago that the atrioventricular nodal recovery curve was dependent on the BCL, an observation that has been reconfirmed in our study (figure 2, *B*). Moreover, after a blocked beat the conduction interval that is observed is larger than that expected from consideration of the recovery curve.

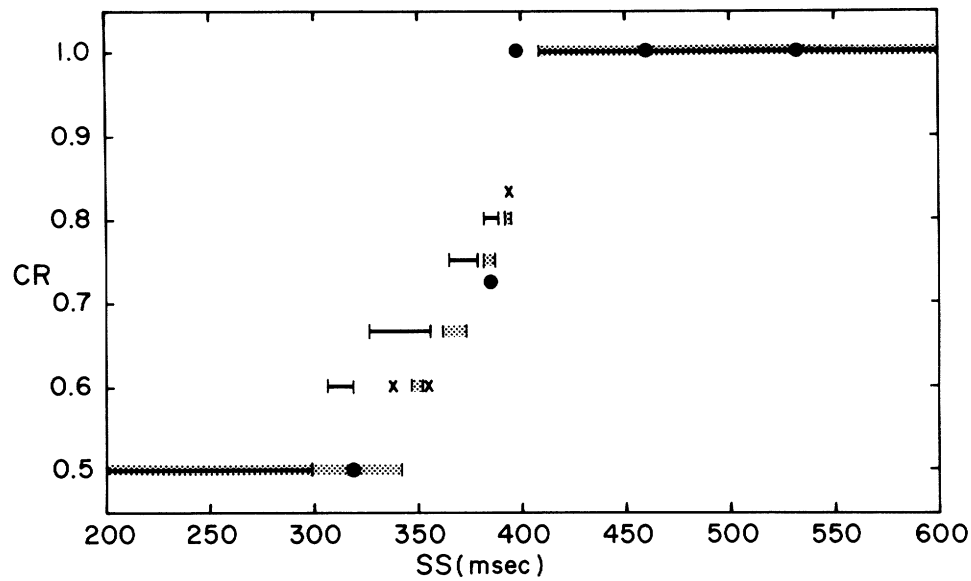

FIGURE 9. CR as a function of SS using the double exponential function as in figure 7 (solid lines) and modified by adding 50 msec to the SH conduction time after a blocked beat (stippled lines). Symbols show observed dynamics as in figure 8. Data are from patient 7.

Thus, the cluster of points in figure 4 that lies off the atrioventricular nodal conduction curve represents the first conducted beat after a blocked beat. The importance of a blocked beat in delaying conduction of the subsequent beat was also well appreciated by Lewis and Master.[15] In addition, there are variations in atrioventricular nodal recovery curves determined after different beats of Wenckebach cycles in dogs.[18] Moreover, there is also a slowly reversible fatigue component that becomes more prominent as stimulation frequency increases.[30] During prolonged periods of rapid stimulation the recovery curve will change and will deviate from one obtained during 1:1 pacing at slower rates. Thus, we would expect a greater deviation between patterns predicted with the use of recovery curves in the 1:1 zone and patterns observed during prolonged rapid pacing.

The effect of the blocked beat on the recovery curve can be readily incorporated in the iterative scheme developed above. Perhaps the simplest way to do this is by adding a constant term to the equation for the recovery curve after a blocked beat. The effects of this modification on the predicted values of the conduction ratio are shown in figure 9. In this patient, the increment in conduction time after a blocked atrial beat is about 50 msec (figure 4). When 50 msec is added to the recovery curve after the blocked beat, there is closer agreement between the predicted and observed conduction ratios than when it is not added (figure 9).

A more accurate theoretical analysis of the effects of the time-dependent changes in the refractory time could be carried out by continually updating the recovery curve used in the theoretical analysis. However, such an analysis would necessarily require determination of the recovery curve after stimulation for various lengths of time. In human beings, such a lengthy procedure is clearly impractical. However, animal experiments show that there is generally an increase in atrioventricular nodal conduction time during the course of periodic stimulation.[30] This gradually increasing conduction time will lead to sequential changes of block, e.g., from 7:6 → 6:5 → 5:4, during the course of a stimulation train in the Wenckebach zone. In fact, as discussed above, such changes in the level of block during stimulation were observed. The refinements that are necessary to represent these time-dependent changes can be incorporated readily into the mathematical formulation, but this was not done in this study.

An interesting question that naturally arises concerns the extent to which the theory presented here accounts for observations of heart block in patients. The analysis can be extended in the following way. A recovery curve can be determined noninvasively from lengthy electrocardiographic recordings in patients with heart block. The recovery curve can then be iterated by the procedures described here. It would then be possible to determine the extent to which the calculations would account for variations in the degree of atrioventricular block that are associated with changes in the sinus rate.[32] However, since other complicating features, such as supernormal conduction[33] and dual

conduction pathways,[34] may be present, extensions of the current analysis will be needed.

We have shown that the atrioventricular nodal recovery curve can be used to compute with reasonable accuracy the sequence and approximate pacing frequencies at which various Wenckebach rhythms are observed. This provides a unified and simple framework for understanding a broad range of rhythms observed during atrioventricular block induced by atrial pacing.

We thank Sandra James and Christine Pamplin for typing the manuscript. We appreciate technical contributions from M. Courtemanche, R. Brochu, and B. Gavin.

References

1. Watanabe Y, Dreifus LS: Atrioventricular block: basic concepts. *In* Cardiac arrhythmias, their mechanisms, diagnosis and management. Philadelphia, 1980, Lippincott, p 406
2. Zipes DP: Second-degree atrioventricular block. Circulation **60:** 465, 1979
3. Berman R: Reverse Wenckebach periods: five cases of an unstable form of partial auriculoventricular block. Am Heart J **50:** 211, 1955
4. Roberge FA, Nadeau RA: The nature of Wenckebach cycles. Can J Physiol Pharmacol **47:** 695, 1969
5. Kosowski BD, Latif P, Radoff AM: Multilevel atrioventricular block. Circulation **54:** 914, 1976
6. Slama R, Leclercq, Rosengarten M, Coumel P, Bouvrain Y: Multilevel block in the atrioventricular node during atrial tachycardia and flutter alternating with Wenckebach phenomenon. Br Heart J **42:** 463, 1979
7. Langendorf R, Pick A: Atrioventricular block, type II (Mobitz)—its nature and clinical significance. Circulation **38:** 819, 1968
8. Guevara MR, Glass L, Shrier A: Phase locking, period doubling bifurcations and irregular dynamics in periodically stimulated cardiac cells. Science **214:** 1350, 1981
9. Glass L, Guevara MR, Belair J, Shrier A: Global bifurcations of a periodically forced biological oscillator. Phys Rev A **29:** 1348, 1984
10. Guevara MR: Chaotic cardiac dynamics, doctoral thesis. McGill University, Montreal, 1984
11. Mobitz W: Uber die unvollständige Störung der Errugungsüberleitung zwischen Vorhof and Kammer des menschlichen Herzens. Zeit Gesamte Exp Med **41:** 180, 1924
12. Decherd GM, Ruskin A: The mechanism of the Wenckebach type of A-V block. Br Heart J **8:** 6, 1946
13. Levy MN, Martin PJ, Edelstein J, Goldberg LB: The AV nodal Wenckebach phenomenon as a positive feedback mechanism. Prog Cardiovasc Dis **16:** 601, 1974
14. Levy MN, Martin PJ, Zieske H, Adler D: Role of positive feedback in the atrioventricular nodal Wenckebach phenomenon. Circ Res **34:** 697, 1974
15. Lewis T, Master AM: Observations upon conduction in the mammalian heart. A-V conduction. Heart **12:** 209, 1925
16. Teague S, Collins S, Wu D, Denes P, Rosen K, Arzabaecher R: A quantitative description of normal AV nodal conduction curve in man. J Appl Physiol **40:** 74, 1976
17. Dresel PE, Man RYK: Prediction of the functional refractory period of the atrioventricular node. J Electrocardiol **11:** 123, 1978
18. Simson MP, Spear JF, Moore EN: Electrophysiological studies on atrioventricular nodal Wenckebach cycles. Am J Cardiol **41:** 244, 1978
19. Billette J: Preceding His-atrial interval as a determinant of atrioventricular nodal conduction time in the human and rabbit heart. Am J Cardiol **38:** 889, 1976
20. Dhingra RC, Rosen KM, Rahimtoola SH: Normal conduction intervals and responses in sixty-one patients using His bundle recording and atrial pacing. Chest **64:** 55, 1973
21. Scherlag BJ, Lau SH, Helfant RH, Berkowitz MD, Stein ES, Damato AN: Catheter technique for recording His bundle activity in man. Circulation **39:** 13, 1969
22. Hoffman BF, Cranefield PF: Electrophysiology of the heart. New York, 1960, McGraw-Hill Book Co.
23. Young M-L, Wholff GS, Castellanos A, Gelband H: Application of the Rosenblueth hypothesis to assess atrioventricular nodal behaviour. Am J Cardiol **57:** 131, 1986
24. Honerkamp J: The heart as a system of coupled nonlinear oscillators. J Math Biol **18:** 69, 1983
25. van der Tweel I, Herbschleb JN, Borst C, Meijler FL: Deterministic model of the canine atrio-ventricular node as a periodically perturbed, biological oscillator. J Appl Cardiol **1:** 157, 1986
26. Landahl HD, Griffeath D: A mathematical model for first degree block and the Wenckebach phenomenon. Bull Math Biophys **33:** 27, 1971
27. Keener JP: On cardiac arrhythmias: AV conduction block. J Math Biol **12:** 215, 1981
28. El-Sherif N, Scherlag BJ, Lazzara R: Pathophysiology of second degree atrioventricular block: a unified hypothesis. Am J Cardiol **35:** 421, 1975
29. Denes P, Levy L, Pick A, Rosen KM: The incidence of typical and atypical A-V Wenckebach periodicity. Am Heart J **89:** 26, 1975
30. Billette J, St. Vincent M: Rate induced fatigue in the rabbit atrioventricular node. Clin Invest Med **8:** B34, 1985
31. Mandelbrot BB: The fractal geometry of nature. San Francisco, 1984, W. H. Freeman and Co.
32. Danzig R, Alpern H, Swan HJC: The significance of atrial rate in patients with atrioventricular conduction abnormalities complicating acute myocardial infarction. Am J Cardiol **24:** 707, 1969
33. Marriot HJ, Conover MH: Advanced concepts in arrhythmias. St. Louis, 1983, CV. Mosby Co.
34. Wu D: Dual atrioventricular nodal pathways: a reappraisal. Pace **5:** 72, 1982